

Effect of Nose Slenderness on Forebody Flow Control

Lars E. Ericsson*

Mountain View, California 94040

and

Martin E. Beyers†

Institute for Aerospace Research, Ottawa, Ontario, K1A 0R6 Canada

When attempting to transfer the forebody flow control technology developed on military aircraft to commercial aircraft, such as the Boeing 1804 SST, additional flow parameters become important. The reason for the complication of the technology transfer is the large difference in forebody slenderness, with apex half-angles below 10 deg in the commercial case compared to above 25 deg for military aircraft. Available experimental results are interpreted on the basis of the existing database for bodies of revolution.

Nomenclature

b	= wing span
c	= reference length, $c = D$
D	= maximum body diameter
l_N	= nose length
M	= Mach number
\dot{m}	= blowing mass flow rate, coefficient $C_\mu = \dot{m}/q_\infty S$
N	= normal force, coefficient $C_N = N/q_\infty S$; $c_n = \partial C_N / \partial \xi$
n	= yawing moment, coefficient $C_n = n/q_\infty S b$
q_∞	= dynamic pressure, $\rho_\infty U_\infty^2 / 2$
Re	= Reynolds number, usually $Re = U_\infty c / \nu_\infty$
r	= local body radius
S	= reference area, projected wing area, $\pi D^2 / 4$ for body alone
t	= time
t^*	= nondimensional time, $x \tan \alpha / r$
U_∞	= freestream velocity
x	= axial distance from the nose
Y	= side force, coefficient $C_Y = Y/q_\infty S$; $c_y = \partial C_Y / \partial \xi$
α	= angle of attack
θ	= direction angle of blowing (Fig. 8)
θ_A	= apex half angle
ν	= kinematic viscosity of air
ξ	= dimensionless x coordinate, $\xi = x/c$
ρ	= density of air
ϕ	= azimuth angle of blowing port (Fig. 8)

Subscripts

A	= apex
max	= maximum
∞	= freestream conditions

Introduction

PREVIOUS studies on fighter aircraft configurations¹ have revealed that forebody flow control devices can generate yaw authority exceeding that of the rudder for angles of attack near maximum lift, typically $\alpha > 30$ deg. Recent tests at low angles of attack of subscale models of a combat aircraft² and a high speed transport configuration^{3,4} were intended to demonstrate the potential for trans-

fer to commercial aircraft of the forebody flow control technology in use on military aircraft. These experiments not only produced an extensive database but also raised many questions. The authors²⁻⁴ found that forebody blowing behaved very differently for the two configurations. Before attempting to transfer existing forebody flow control capability for use on commercial aircraft the all-important influence of forebody slenderness on asymmetric flow separation characteristics^{5,6} has to be taken into account.

Background

In Ref. 2 the pneumatic vortex control (PVC) devices were investigated on a 6% scale model of the F-16 forebody. The tests were performed at $0 \leq \alpha \leq 18$ deg, $M = 0.8$, and $Re = 0.85 \times 10^6$ based on the maximum forebody cross-section dimension (Fig. 1). An analysis⁵ of experimental results for sharp tangent ogive, sharp cone, paraboloid, blunt tangent ogive, and blunt cone geometries⁷ shows that as long as the crossflow Mach number $M_\infty \sin \alpha$ does not exceed 0.4 there are no apparent compressibility effects on the crossflow separation characteristics. Consequently, as the experimental results in Fig. 1 are for $\alpha < 30$ deg, they are of incompressible nature and can be compared with the low speed results for the Boeing SST aircraft.³ Figure 1 shows that the desired linear C_n dependence on the blowing rate was obtained. However, the response at $\alpha = 15$ deg for $C_\mu = 0.004$ was only equivalent to a 5-deg rudder deflection on the full-scale aircraft.⁴ Of course, with the apex half-angle $\theta_A > 25$ deg, the forebody crossflow was still attached at $\alpha < 25$ deg,⁵ and the blowing only tilted the boundary layer displacement surface to generate the side force on the forebody that produced the measured C_n response. These test results did not give any indication of what would happen when the same PVC geometry was applied to a 3% scale model of the Boeing 1804 SST aircraft³ (Fig. 2), which has a much more slender nose than the F-16, $\theta_A < 10$ deg compared to $\theta_A > 25$ deg, respectively.

The results³ in Fig. 3 show that at $\alpha = 4$ deg, i.e., for $\alpha/\theta_A < 0.5$, the $C_n(C_\mu)$ characteristics were linear, as observed earlier for the F-16 forebody at a $\alpha \leq 18$ deg, i.e., for $\alpha/\theta_A < 1$ (Fig. 1). However, when the angle of attack was increased to $\alpha = 12$ deg, i.e., $\alpha/\theta_A > 1.2$, the magnitude of the $C_n(C_\mu)$ slope was initially, at $C_\mu \leq 0.0004$, one order of magnitude larger than at $\alpha = 4$ deg. Although the difference in slot length, 8 in. at $\alpha = 4$ deg compared to 1 in. at $\alpha = 12$ deg, could have had some effect, the main reason is that $\alpha = 12$ deg is in the range $1 < \alpha/\theta_A < 2$, where symmetric forebody crossflow separation occurs in the absence of blowing.⁵ The modest blowing rate $C_\mu = 0.0004$ was enough to cause a change to asymmetric crossflow separation. One expects that even lower blowing rates would be required at higher α until $\alpha/\theta_A \geq 2$, where the blowing has to overcome the effect of nose microasymmetry.^{5,6} Once this change from symmetric to asymmetric crossflow separation had taken place, however, the $C_n(C_\mu)$ slope for $C_\mu > 0.0004$

Presented as Paper 98-0499 at the AIAA 36th Aerospace Sciences Meeting and Exhibit, Reno, NV, 12–15 January 1998; received 1 April 1998; revision received 18 March 1999; accepted for publication 22 March 1999. Copyright © 1999 by Lars E. Ericsson and Martin E. Beyers. Published by the American Institute of Aeronautics and Astronautics, Inc., with permission.

*Engineering Consultant, 1518 Fordham Way, Fellow AIAA.

†Head Aircraft Aerodynamics, Applied Aerodynamics Laboratory, Senior Member AIAA.

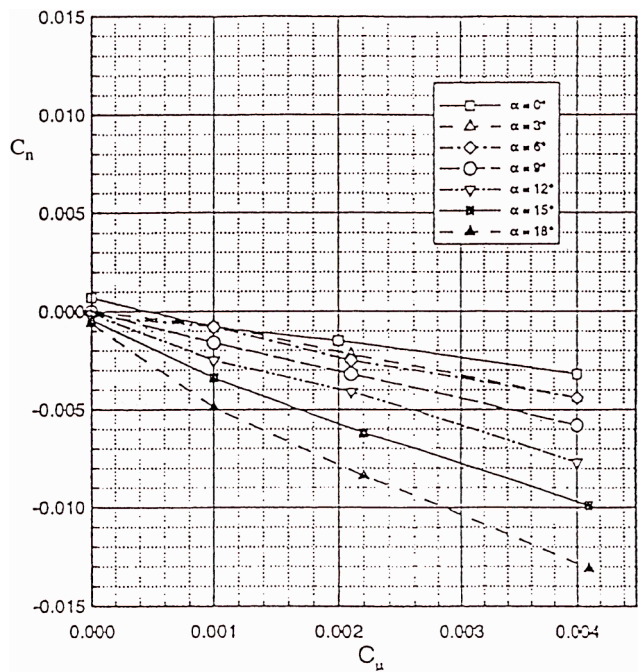


Fig. 1 Pneumatic vortex control (PVC) at $M = 0.8$ on a 6% scale model of the F-16 forebody.²

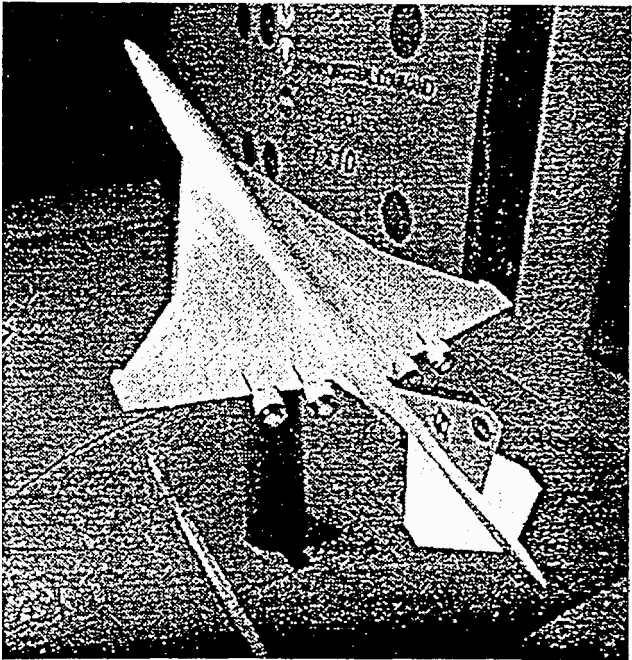


Fig. 2 3% scale model of the Boeing 1804 SST aircraft.³

was of the same modest magnitude as for $\alpha = 4$ deg. This initially very large effect of blowing, preventing the establishment of the desired linear $C_n(C_\mu)$ characteristics, is caused by the bistable character of the crossflow separation asymmetry.⁵ It is a general problem in forebody flow control.⁶ One solution to this problem has been described,⁸ i.e., to control the time duration of the bistable left- and right-hand asymmetric separation configurations. As this type of control is likely to have a feedback loop, it solves the problem of the lateral movement of the crossflow stagnation point on a maneuvering combat aircraft, which most conventional forebody control devices¹ are subject to.⁹

SST Configuration

The experimental results³ for $C_\mu = 0.0040$ in Fig. 4 show control reversal to occur at $\alpha > 10$ deg, and the data in Fig. 5 demonstrate

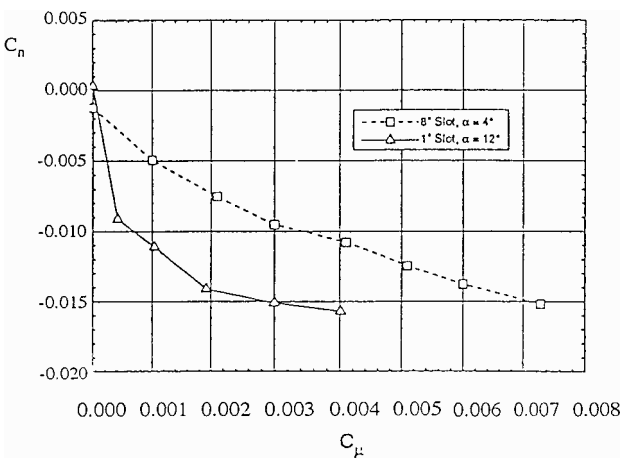


Fig. 3 Effect of asymmetric slot blowing on SST model at $\alpha = 4$ and 12 deg (Ref. 3).

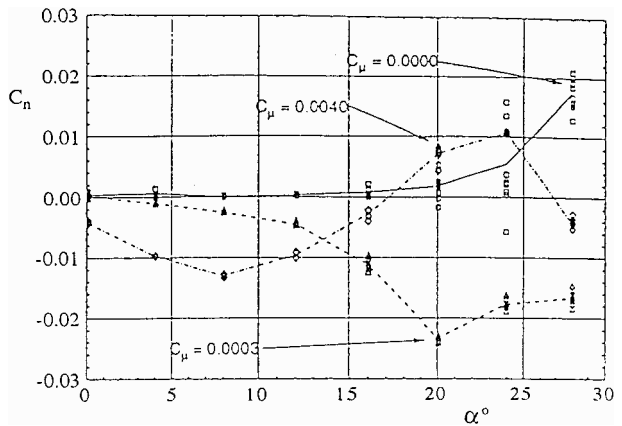


Fig. 4 Sensitivity to angle of attack of the effect of asymmetric blowing by 1-in. slot at the most forward location on SST model.³

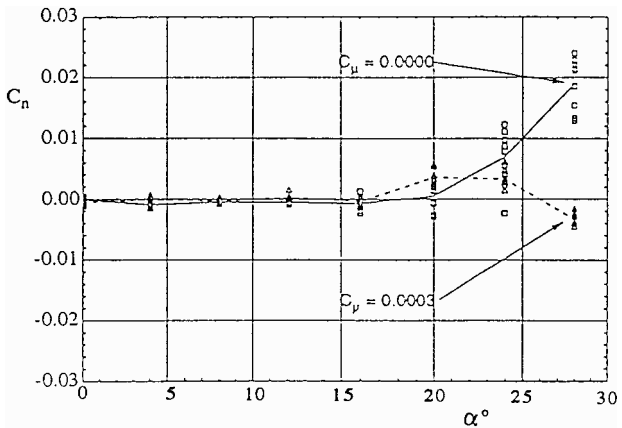


Fig. 5 Effect of symmetric blowing by the 1-in. slot geometry (1/0) on $C_n(\alpha)$ for SST model.³

that symmetric blowing of very modest magnitude, $C_\mu = 0.0003$, can eliminate the effect of nose microasymmetry⁵ at $\alpha > 20$ deg ($C_\mu = 0$). To understand these characteristics one needs to revisit the database for ogive-cylinder and cone-cylinder bodies.^{5,6} The incompressible experimental results¹⁰ in Fig. 6 for $\alpha = 50$ deg illustrate the great sensitivity to Reynolds number of the crossflow separation at $\alpha/\theta_A = 1.8$ and indicate that the SST will have a multicellular type of forebody crossflow separation at $\alpha \geq 18$ deg. As is discussed in detail in Ref. 5, the crossflow characteristics of a circular cylinder change dramatically with Reynolds number,¹¹ the symmetric, critical crossflow separation geometry giving the minimum drag.

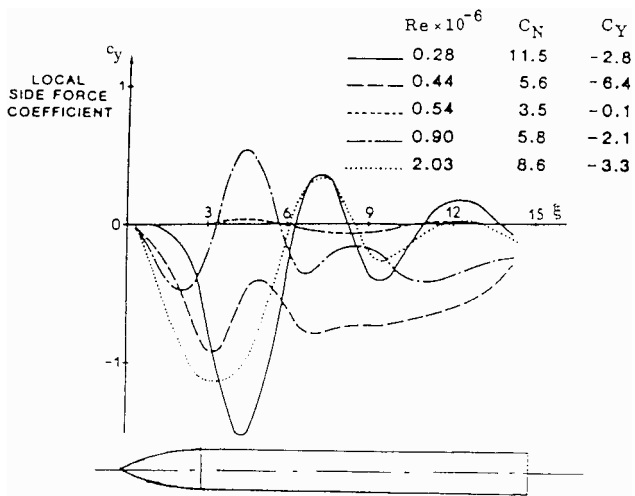


Fig. 6 Side-force distribution at $\alpha = 50$ deg on an ogive-cylinder through the critical Reynolds number range.¹⁰

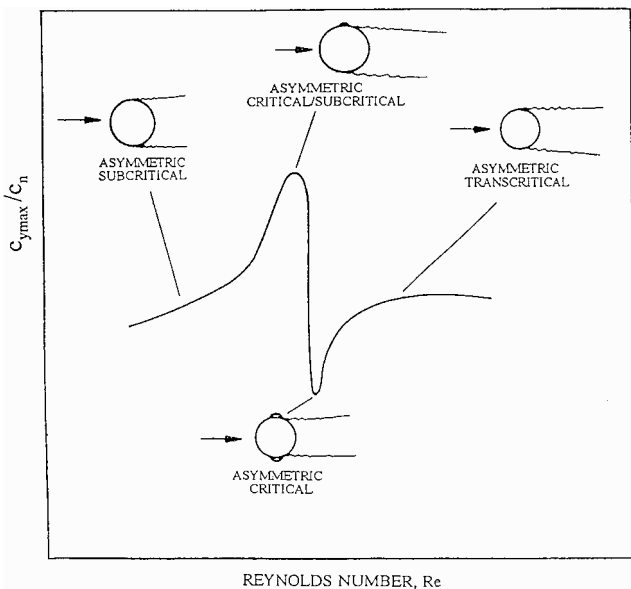


Fig. 7 Expected effects of flow-separation type on the normalized side force.⁵

Accordingly, the asymmetric crossflow separation on an inclined body of revolution will change with Reynolds number as illustrated⁵ in Fig. 7, showing that both the maximum and minimum local side-force/normal-force ratio can be established in the critical Re range. This is demonstrated by the experimental results¹⁰ in Fig. 6, where the maximum $|C_Y|/C_N$ ratio occurred at $Re = 0.44 \times 10^6$ and the minimum at $Re = 0.54 \times 10^6$, where Re is based on the maximum body diameter. As the tests of the SST model^{3,4} were performed at $Re = 0.51 \times 10^6$, based on the maximum forebody diameter, the crossflow conditions were in the critical range and the flow conditions producing the minimum side force on the forebody could be established. This explains why in Fig. 5 symmetric blowing at the miniscule rate $C_\mu = 0.0003$ could result in the elimination of the yawing moment generated by nose microasymmetry effects⁵ at $C_\mu = 0$.

The nonblowing slot and nozzle geometries for forebody blowing on the 3% scale model of the Boeing 1804 SST model³ (Fig. 8) generated a nose microasymmetry different from that on the clean model, judging by the experimental results⁴ in Fig. 9. Blowing orifices on a 5-deg cone presented similar deviation from the asymmetric flow characteristics for the clean model.¹² This microasymmetry effect of the nozzle at $\xi = 1.0$ from apex and $\theta = 30$ deg (Figs. 8 and 9) was overpowered by blowing at $C_\mu = 0.0020$, producing C_n

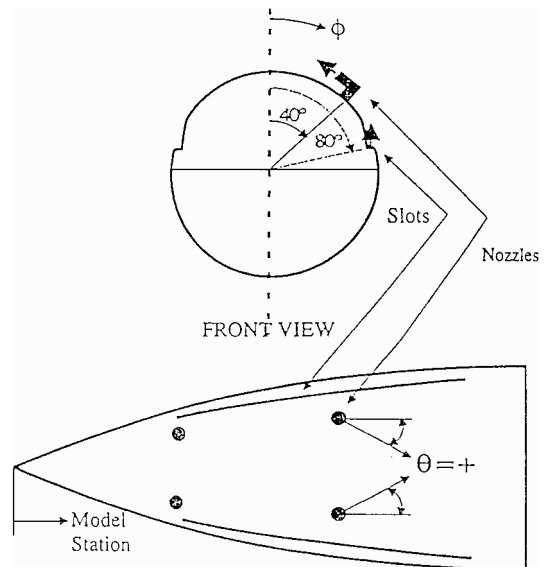


Fig. 8 PVC slot and nozzle orientation on the SST model.³

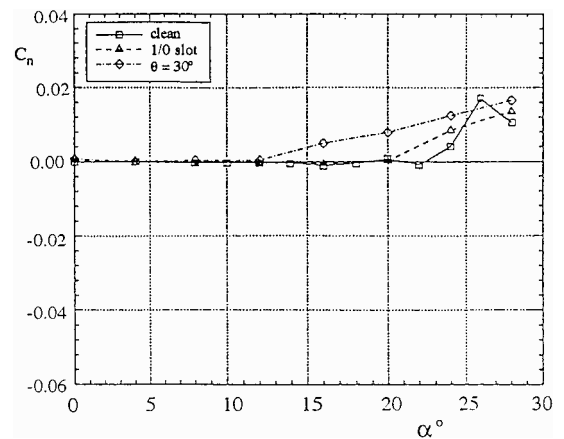


Fig. 9 Microasymmetry effect of nonblowing slot or nozzle.⁴

of similar magnitude on the left- and right-hand side of the forebody³ (Fig. 10). At $C_\mu = 0.0040$ the effect of moving the 1-in. slot (Fig. 8) progressively aft on the forebody³ (Fig. 11a) was insignificant until $\alpha > 10$ deg, i.e., $\alpha/\theta_A > 1$, where asymmetric blowing can cause the symmetric crossflow separation to become asymmetric.^{5,6} Moving the 2-in. slot had a similar effect (Fig. 11b). (Slot configurations were designated by the slot length and location, e.g., 2/4 is a 2-in. slot 4 in. aft of the most forward location possible.) It is noteworthy that in the most forward location both slot lengths (1/0 in Fig. 11a and 2/0 in Fig. 11b) produced control reversal, giving $C_n > 0$ for $\alpha > 17$ deg, i.e., for $\alpha/\theta_A > 1.7$, and both generated very similar $C_n(\alpha)$ trends for slot locations 2 and 4 (or more) in. aft (1/2 and 2/4 in Figs. 11a and 11b, respectively).

The large effect of slot location, as well as the control reversal in Figs. 4 and 11, can be explained on the basis of results obtained on missile bodies.⁵ The experimental results¹⁰ in Fig. 6 show how increasing the supercritical Reynolds number, $Re > 0.54 \times 10^6$, started the development of a side force closer and closer to the nose apex, resulting in a multicellular side-force distribution. The experimental results for an $L_N/D = 2.5$ ogive-cylinder³ in Fig. 12a show that the side-force distribution moved closer and closer to the nose tip also when the angle of attack is increased at a constant Reynolds number. The results in Fig. 12a were shown to collapse on one curve when applying the impulsive flow analogy for slender bodies¹⁴ and plotting the local side force as a function of the dimensionless time $t^* = x \tan \alpha / r$ (Fig. 12b). Also, boundary layer blowing can affect flow separation in a way that in many aspects is

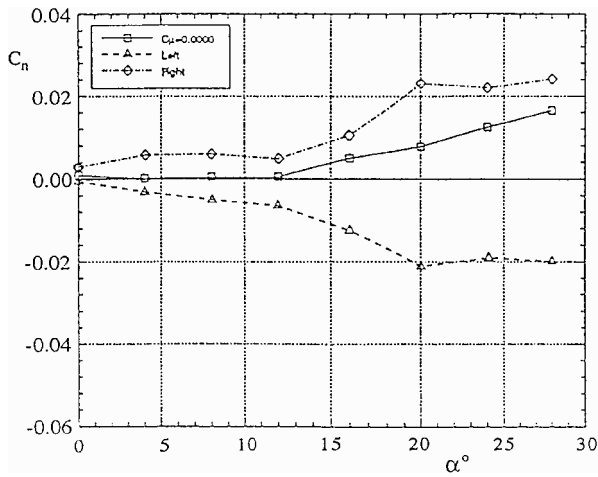
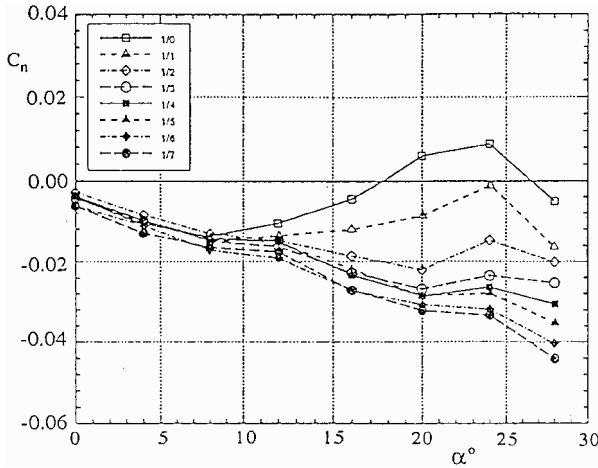
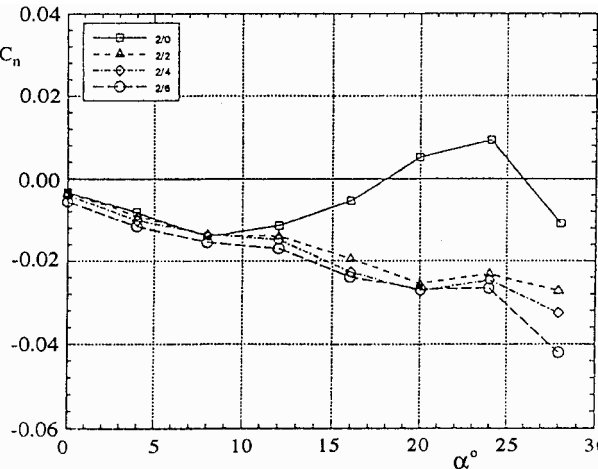


Fig. 10 Capability of $C_\mu = 0.0020$ left- and right-side nozzle blowing (at $\theta = 30$ deg at the 1-in. location) to overpower the nozzle microasymmetry effect.⁴



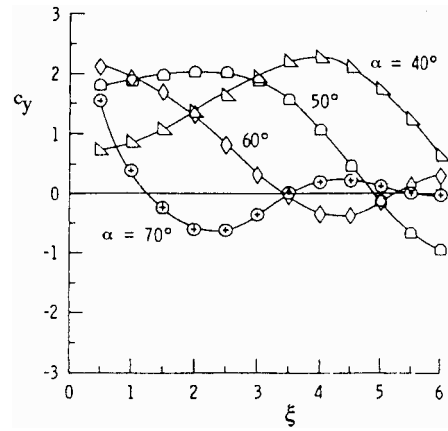
a) 1-in. slot



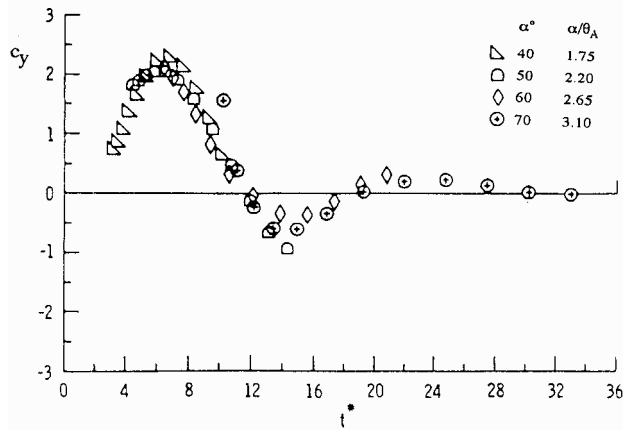
b) 2-in. slot

Fig. 11 Influence of axial slot location on the effect of $C_\mu = 0.0040$ blowing.⁴

similar to the effects of changing the Reynolds number, increasing blowing being somewhat equivalent to increasing the supercritical Reynolds number (Fig. 6). Thus, when in Fig. 4 the blowing was increased from $C_\mu = 0.0003$ to 0.0040 , the side-force distribution would be expected to change in a manner similar to that when the Reynolds number is increased in Fig. 6, say from $Re = 0.44 \times 10^6$ to 0.90×10^6 . This would change the resulting yawing moment dramatically, explaining the data trend for $C_\mu = 0.0040$ in Fig. 4, where



a) c_y as a function of axial position



b) c_y as a function of nondimensional time

Fig. 12 Local side-force distribution for $l_N/D = 3.5$ tangent-ogive cylinder at $Re = 0.2 \times 10^6$ (Ref. 13).

the blowing effect on C_n even reverses its trend when $\alpha > 10$ deg, i.e., $\alpha/\theta_A > 1$. In this high alpha range the blowing controls the separation asymmetry.

Moving the blowing slot aft (Figs. 11a and 11b) would increase the length of the first asymmetric load cell, an effect similar to that of decreasing the Reynolds number in Fig. 6 from $Re = 0.90 \times 10^6$ to 0.44×10^6 , for example. The experimental results in Fig. 6 for the effect of Reynolds number on the side-force distribution on bodies of revolution qualitatively illustrate the potential effect of changing the slot location for blowing at critical crossflow conditions on the SST model (Figs. 11a and 11b).

In the case of advanced fighter aircraft, such as the F-16, where the effective apex half-angle is larger than 25 deg, the natural cross-flow asymmetry is delayed to $\alpha \geq 50$ deg, and any multicellular side-force distribution can only be established at very high angles of attack, e.g., at $\alpha = 60$ and 70 deg in Fig. 12a. The onset of asymmetric flow separation is delayed further by the upwash induced by Leading Edge Extension surfaces (LEXs) in the case of the F-16 aircraft.^{15,16} Thus, the application of forebody flow control to combat aircraft is much simpler than in the case of a commercial aircraft configuration, such as the SST discussed here, where the slender forebody will produce a multicellular side-force distribution in the angle-of-attack range of practical interest for takeoff and landing. This makes the design of a successful forebody flow control mechanism more difficult than in the case of fighter aircraft.

Conclusions

An analysis of published experimental and theoretical results has shown why the transfer of forebody flow control technology from military to commercial aircraft is not simple. However, the experimentally observed forebody control performance can be explained on the basis of existing knowledge of high-alpha flows on bodies

of revolution. Consequently, the conclusion to be drawn from this exploratory analysis is that the potential benefits are likely to justify the further research and development that will be needed before successful commercial use of forebody flow control will be possible.

References

- ¹Malcolm, G., "Forebody Vortex Control—A Progress Review," AIAA Paper 93-3540, Aug. 1993.
- ²Eidson, R. C., and Mosbarger, N. A., "Forebody Pneumatic Devices at Low Angles of Attack and Transonic Speed," AIAA Paper 97-0042, Jan. 1997.
- ³Takahashi, T. T., Eidson, R. C., and Heineck, J. T., "Aerodynamic Characteristics of a Supersonic Transport with Pneumatic Flow Control," AIAA Paper 97-0043, Jan. 1997.
- ⁴Parker, B. A., Eidson, R. C., and Takahashi, T. T., "Forebody Vortex Flow Control on a High Speed Transport Configuration," AIAA Paper 97-0044, Jan. 1997.
- ⁵Ericsson, L. E., and Reding, J. P., "Asymmetric Flow Separation and Vortex Shedding on Bodies of Revolution," *Tactical Missile Aerodynamics, General Topics*, Vol. 141, edited by M. J. Hemsch, Progress in Astronautics and Aeronautics, AIAA, Washington, DC, 1992, Chap. 10, pp. 391-452.
- ⁶Ericsson, L. E., "Control of Forebody Flow Asymmetry—A Critical Review," AIAA Paper 90-2833, Aug. 1990.
- ⁷Wardlaw, A. B., Jr., and Morrison, A. M., "Induced Side Forces at High Angles of Attack," Naval Surface Warfare Center/WOL, TR-75-176, Dahlgren, VA, Nov. 1975.
- ⁸Lee, R., Hanff, E. S., and Kind, R. J., "Linear Control of Side Forces and Yawing Moments Using the Dynamic Manipulation of Forebody Vortices," International Council of the Aeronautical Sciences, ICAS 96-2.10.1, Sept. 1996.
- ⁹Ericsson, L. E., and Beyers, M. E., "Conceptual Fluid/Motion Coupling in the Herbst Supermaneuver," *Journal of Aircraft*, Vol. 34, No. 3, 1997, pp. 271-277.
- ¹⁰Champigny, P., "Reynolds Number Effect on the Aerodynamic Characteristics of an Ogive-Cylinder at High Angles of Attack," AIAA Paper 84-2176, Aug. 1984.
- ¹¹Achenbach, E., "Influence of Surface Roughness on the Cross Flow Around a Circular Cylinder," *Journal of Fluid Mechanics*, Vol. 46, Pt. 2, 1971, pp. 321-335.
- ¹²Peake, D. J., and Owen, F. R., "Control of Forebody Three-Dimensional Flow Separation," Paper 15, AGARD CP-262, 1979.
- ¹³Hall, R. M., "Forebody and Missile Side Forces and the Time Analogy," AIAA Paper 87-0327, Jan. 1987.
- ¹⁴Sarpkaya, T., "Separated Flow About Lifting Bodies and Impulsive Flow About Cylinders," *AIAA Journal*, Vol. 4, No. 3, 1966, pp. 414-420.
- ¹⁵Beyers, M. E., and Ericsson, L. E., "Unsteady Aerodynamics of Combat Aircraft Maneuvers," AIAA Paper 97-3647, Aug. 1997.
- ¹⁶Ericsson, L. E., and Beyers, M. E., "Wind Tunnel Aerodynamics in Rotary Tests of Combat Aircraft," *Journal of Aircraft*, Vol. 35, No. 4, 1998, pp. 521-528.